



Original article

The mechanism of lipopolysaccharide administration-induced cognitive function impairment caused by glucose metabolism disorder in adult rats

Yiri Du^a, Hongwei Cui^c, Yunfeng Xiao^e, Jianbo Li^d, Engboer Su^b, Zhipeng Xu^{a,*}, Weidong Mi^{a,*}^aAnesthesiology and Operation Center, The General Hospital of the People's Liberation Army, Beijing 100853, China^bAnesthesiology Department, Affiliated Hospital of Inner Mongolia Medical University, Hohhot 010050, China^cClinical Medical Research Center, Affiliated Hospital of Inner Mongolia Medical University, Hohhot 010050, China^dNuclear Medicine Department, Affiliated Hospital of Inner Mongolia Medical University, Hohhot 010050, China^eNew Drug Safety Evaluation and Research Center, Inner Mongolia Medical University, Hohhot 010110, China

ARTICLE INFO

Article history:

Received 3 April 2019

Revised 26 June 2019

Accepted 30 June 2019

Available online 2 July 2019

Keywords:

Postoperative cognitive dysfunction

Surgical trauma

Glucose metabolism

18F-FDG PET/CT

PI3K, IRS-2, AKT, and GLUT4 pathway

ABSTRACT

Objective: This essay aims to make investigation on the mechanism of glucose metabolism disorder and Lipopolysaccharide administration-induced cognitive function impairment in adult rats with surgery. **Methods:** Divide the objects, 40 male Sprague-Dawley rats at the age of 9 months, into 4 groups. Provide unilateral nephrectomy surgery and/or lipopolysaccharide intraperitoneal injection. Postoperative cognitive function evaluation would be tested by the Morris water maze. Rats with Postoperative Cognitive Dysfunction (POCD) were scanned to analyze the brain glucose metabolism by means of 18F-FDG PET/CT. Phosphatidylinositol 3-Kinase (PI3K), Protein Kinase β (AKT), Insulin Substrates Receptor-2 (IRS-2) and Glucose Transporter 4 (GLUT4) were detected as well. Data will be captured through gene expression in POCD rats via Quantitative Real-Time PCR (QRT-PCR). On the other side, Western Blot was used to measure the expression levels of IRS-2, p-IRS-2, p-PI3K, PI3K, p-AKT, AKT, GLUT4, and p-GLUT4. **Results:** During the Morris water maze test, the staging time (latency) of rats in each group was becoming short gradually as the training progressed. The incubation time of Day 5 of each group was shorter than that of Day 1 ($P < 0.05$). On the Day 3 after the surgery, the average target quadrant residence time of Group S+L (100 $\mu\text{g}/\text{Kg}$) was shorter, compared with Group C, L and S. Of which, the average number of perforation was reduced greater than that of Group C ($P < 0.05$). The average swimming speed of the groups is of no distinct difference ($P > 0.05$). After the operation, there was no great difference shown among the subjects ($P > 0.05$) in the average residence time of the target quadrant, the mean number of passages, and the mean swimming speed. On Day 3, the average latency of Group S+L (100 $\mu\text{g}/\text{Kg}$) was longer than Group C ($P < 0.05$) in the working memory test after the operation. The average latency of rats in Group L and S was showed longer than that in Group C, with tiny difference ($P > 0.05$). In the 7-Day working memory test, the average latency of the rats in Group L, S and S+L (100 $\mu\text{g}/\text{Kg}$) was obviously longer than that in Group C. Comparing to preoperative rats, POCD rats of Group S+L (100 $\mu\text{g}/\text{Kg}$) were scanned by 18F-FDG PET/CT three days later after the operation. Its SUVmax of the frontal and temporal lobe areas were decreased significantly ($P < 0.05$). However, difference degree was not significantly shown in the SUVmax between Group C and the preoperative rats ($P > 0.05$). In comparison with the gene expression of of Group C, the PI3K, IRS-2, AKT and GLUT4 mRNA genes are the key genes in the insulin signaling pathways of the hippocampus of the POCD rats.

Abbreviations: AGE, Advanced Glycation End products; FDG, Fluorodeoxyglucose; IRS-2, Insulin Substrate Receptor-2; GLUT4, Glucose Transporter 4; LPS, Lipopolysaccharide; MAPK, Mitogen-Activated Protein Kinase; ROS, Reactive Oxygen Species; SUV, Standard Uptake Value; TLR4, Toll-like Receptor 4; OSEM, Ordered Subsets Expectation Maximization; PI3K, Phosphatidylinositol 3-Kinase; POCD, Postoperative Cognitive Dysfunction; QRT-PCR, Quantitative Real-Time PCR.

* Corresponding authors.

E-mail addresses: xuzhipeng20@163.com (Z. Xu), mwd1962@sina.cn (W. Mi).

Peer review under responsibility of King Saud University.

<https://doi.org/10.1016/j.sjbs.2019.06.017>

1319-562X/© 2019 The Authors. Production and hosting by Elsevier B.V. on behalf of King Saud University.

This is an open access article under the CC BY-NC-ND license (<http://creativecommons.org/licenses/by-nc-nd/4.0/>).

The expression level was reduced. The expression level of all protein of PI3K, IRS-2, GLUT4 and AKT in the POCD rats was of no great contrast with that in Group C. But for IRS-2 protein, the phosphorylation level has increased, and meanwhile decreased for AKT, PI3K and GLUT4 proteins ($P < 0.05$). Conclusions: Adult SD rats cognitive dysfunction model treated with unilateral nephrectomy combined and 100 $\mu\text{g}/\text{kg}$ LPS intraperitoneal injection were led to abnormal both brain glucose metabolism and insulin expression. The proved phenomenal results signal pathway-related proteins PI3K, IRS-2, AKT and GLUT4. It reached the conclusion that surgical trauma, rather than anesthesia, leads to impaired cognitive function. PI3K, IRS-2, AKT, and GLUT4 pathway of brain can be partial explanations of the pathogenesis of POCD.

© 2019 The Authors. Production and hosting by Elsevier B.V. on behalf of King Saud University. This is an open access article under the CC BY-NC-ND license (<http://creativecommons.org/licenses/by-nc-nd/4.0/>).

1. Introduction

After a major surgery, a central nervous system complication often occurs, which is called as POCD, the Postoperative Cognitive Dysfunction. Clinical manifestations normally include the loss of learning ability, memory, thinking ability and executive and expression ability (Feinkohl et al., 2017a; Needham et al., 2017). POCD may last from a few hours, to a few days or weeks after surgery. In some cases, the disorder may exist for a few months, or even be permanent. Thus, it will result in reducing medication compliance, prolonging hospital stay, and increasing patients' costs, etc. (Carr et al., 2018). With the rising number of surgery patients; the quantity of patients suffered from POCD is increasing year by year. Therefore, finding effective methods to treat POCD has become a thorny problem. The specific pathogenesis and mechanism of POCD remains unclear. Most scholars believe that POCD is caused by the degeneration of central nervous system in elder patients and induced by surgery and anesthesia. The brain energy metabolism disorder is caused by a combination of various risk factors and leads to neurological dysfunction (Casella and Bimonte, 2017; Cropsey et al., 2015; Steinmetz and Rasmussen, 2016). Perioperative patients often have fluctuations in blood glucose, which might be accompanied by high and low blood glucose levels, and the postoperative brain glucose uptake rate of POCD patients is significantly reduced. Recent studies have also found that hyperglycemia during extracorporeal circulation is a risk factor for POCD (Feinkohl et al., 2017b; Jones, 2008). Therefore, study on the mechanism of POCD caused by abnormal glucose metabolism is of important guiding significance for perioperative clinical intervention. Studies have shown that glucose metabolism disorder is an important pathological mechanism of cognitive impairment (Díaz-Venegas et al., 2017). McNay et al. found that hippocampal-dependent learning and memory function is related to brain glucose metabolism using brain microdialysis technique (McNay and Recknagel, 2011). The mechanisms of abnormal glucose metabolism leading to POCD involve increased insulin resistance, abnormal insulin signaling pathway, enhanced oxidative stress response, increased advanced glycation end products (AGE), abnormal blood-brain barrier, and glucose transporter-4 metabolic disorders, among which, the insulin signaling pathway IRS-PI3K-AKT-GLUT4 disorder may exert influence on neuronal glucose metabolism and cognitive function changes (Rizzo et al., 2014; Pearson-Leary and McNay, 2016; Yaffe et al., 2011).

At present time, diagnosis methods for POCD is insufficient. 18F-FDG (18F-fluorodeoxyglucose) PET/CT is an effective approach in detecting brain glucose metabolism-related damage in neurodegenerative dementia. Normal brain cells have high metabolism rate of 18F-FDG uptake, with standard uptake value. Standard Uptake Value (SUV) is a quantitative indicator that reflects the level of glucose concentration in brain cells, which functionally reflects the metabolic level of brain cells (Banzo et al., 2014; Jiménez-Bonilla et al., 2016). In addition, lipopolysaccharide (LPS) is the main bacterial toll-like receptor 4 (TLR4) ligand that actuates the immune

system to respond to infection. Previous studies have shown that surgery in adult rats with intraperitoneal injection of LPS might trigger more serious neurodegenerative diseases, which suggests that adult rats are more prone to cognitive disorders when they have received surgery. This simulates the cognitive function of surgical infection status in young patients in clinical settings (Sochocka et al., 2017; Fischer et al., 2011). In this study, adult rats that have unilateral nephrectomy and have been treated with LPS intraperitoneal injection were used to cause adult rat cognitive dysfunction model. 18F-FDG PET/CT photo copies were used to record and test the changing of brain glucose metabolism of the rats with cognitive dysfunction. Molecular biological techniques were adapted to detect the changes of INSR-PI3K-AKT-GLUT4 of the insulin signaling pathway. Apart from the above, those techniques were helpful to explain the mechanism of glucose metabolism changes of POCD in adult rats, and to provide reference for preventing and treating POCD.

2. Experimental materials & methods

2.1. Objects/animals

Forty 9-month male Sprague-Dawley (SD) rats, ranging among 400–430 g, were caught from Vitallihua Experimental Animal Technology Co., Ltd. (license number: SCXK (Beijing) 2012-0001). Experimental objects were kept in SPF room of the Experimental Animal Center, Inner Mongolia Medical University. The room temperature was controlled at a suitable temperature ($23 \pm 1^\circ\text{C}$) to simulate the circadian rhythm. The warm fluorescent lamp was automatically switched on every 12 h. Food and water were offered sufficiently and accordingly. All the experimental rats were kept in the set environment for 7 days to get used to. The animal experiment was permitted by the Animal Ethics Committee, the General Hospital of the People's Liberation Army. Meanwhile, all guidelines of the National Institute of Health was followed strictly during the process of carrying out animal feeding and experimental operations to minimize the damage suffered by the experimental animals. Forty rats were divided into 4 groups randomly. *The control group* (Group C, $n = 10$): receiving intraperitoneal injection of placebo (0.3 mL normal saline) on the day of the surgery; *LPS intraperitoneal injection group* (Group L, $n = 10$): receiving LPS 100 $\mu\text{g}/\text{kg}$ on the day of the surgery; *surgery group* (Group S, $n = 10$): receiving unilateral nephrectomy surgery; *surgery + LPS intraperitoneal injection group* (Group S+L, $n = 10$): receiving intraperitoneal injection of LPS 100 $\mu\text{g}/\text{kg}$ 1 h before the surgery, followed by unilateral nephrectomy surgery.

2.2. Experimental instruments and reagents

Morris water maze and analysis software is provided by Inner Mongolia University. Siemens Inveon PET/CT and Minitrace type cyclotron is provided by the Nuclear Medicine Department,

Affiliated Hospital of Inner Mongolia Medical University. Germany SIGMA 3K15 high-speed refrigerated centrifuge, American ThermoFisher NanoDrop 2000 nucleic acid protein, and the analyzer, the American ABI 7500 fluorescence quantitative PCR instrument, as well as the US GENE Li-COR far infrared laser scanning system (ODYSSEY) are all provided by the Clinical Medical Research Center, Affiliated Hospital of Inner Mongolia Medical University.

Lidocaine Hydrochloride Injection was from Shandong Hualu Pharmaceutical Co., Ltd. Pentobarbital Sodium was from National Pharmaceutical Group Chemical Reagent Co., Ltd. Lipopolysaccharide (LPS) was purchased from SIGMA, USA. In the experiment, RIPA lysate (Solarbio), PC0020 BCA protein quantification kit (Solarbio), and WB antibody (Cell Signalling, USA) were also applied.

2.3. Experimental method

2.3.1. The model adult rats treated with surgery and lipopolysaccharide

All rats were trained for water maze navigation task for five days before the surgery. One hour before the surgery, each group was given intraperitoneal injection of the corresponding dose of the drug. One hour later, the Group S and Group S+L were given unilateral nephrectomy surgery. Behavioral tests were performed during post-surgery period of 3 days after and 7 days respectively.

The establishment of this model mimics the human surgery and clinical infection status. First, Group S+L was given LPS (100 µg/kg) intraperitoneally 1 h before the surgery. One hour later, Group S were given a left hepatectomy surgery under general anesthesia condition. 10% Sodium pentobarbital solution (0.3 mL/100 g) was intraperitoneally injected during the surgery. After the righting reflex disappeared, the left lower costal abdomen was shaved, and the lateral position was fixed on the disinfection operating table. After the conventional iodophor disinfection was done, a towel with a sterile hole was placed on the table, and a longitudinal incision was made about 3–4 cm to the midline of the left rib margin. The kidney was inserted into the abdominal cavity to reveal the renal pedicle. The renal artery was ligated at both the distal and proximal ends of the renal hilum. Then, the renal artery, renal vein and ureter were ligated, and the left kidney was completely removed. Then after the blood stanching, the surgical wound should be stitched back. The whole operation should be carried under aseptic conditions. After warmed up, SD rats recovered from righting reflex, and were taken back to the breeding room for feeding, and the behavioral tests were performed 3 and 7 days after the surgery respectively. The use of longitudinal incision on the back prevents the rat from biting its own wound during daily activities.

2.3.2. Morris Water Maze test

One common tool for studying behavioral neuro-science is the Morris Water Maze test, which is often used to assess the effects of neuro-cognitive therapy in rats. The experiment is divided into 2 phases, learning phase and memory phase. The learning phase is designed to last for one week. Before starting the experiment, the rats should be placed in a room with the water maze to make sure that they can fully adapt to the environment. The Morris water maze is a 51 cm-tall black and non-reflective stainless-steel drum, with a diameter of 210 cm. It is fixed in a quiet room with dim light. The barrel is filled with clean and tasteless warm water, of which the depth is 40 cm and the temperature is controlled at 24 ± 1 °C. The light for the camera probe to detect the SD rats is controlled strictly. The labyrinth pool is allocated into four quadrants, I, II, III, and IV. A circular underwater escape platform was placed in the first quadrant with a platform of 15 cm-diameter and 1 cm-lower below the water surface. During the experiment, all markers were set in fixed position. The experiment

was carried at the same time every day. The camera was set directly above the pool to record the trajectory of the aged SD rats. The data collection and data processing were performed by Beijing Dingda Water Labyrinth Software. The experiment is divided into three parts: positioning navigation experiment, space exploratory experiment and working memory detection.

2.3.3. Small animal PET-CT scan of glucose metabolism in brain of POCD rats

PET/CT scans of small animals' brain were performed on POCD rats and normal rats to obtain records of changing of brain glucose metabolism. Rats received injection of 18F-FDG for 40 min. The rats were then taken to the small animals PET/CT to receive brain scan. Before the PET/CT scan, the rats were anesthetized with a 10% chloral hydrate solution at a ratio of 3 mL/Kg, and fixed in the prone position. Scanning process: firstly, it would take to perform 5 min Micro-CT image, then PET image was done in 10 min, and then the images were captured through the SIEMENS Inveon MM workstation with Ordered Subsets Expectation Maximization (OSEM). Images of CT, PET, and fusion of the rat brain were obtained respectively. Quantitative analysis data of 18F-FDG uptake by POCD rat brain cells were obtained by SIEMENS Inveon MM IRW image fusion software.

2.3.4. The gene and protein expression of *INSR*, *PI3K*, *p-PI3K*, *p-AKT*, *AKT*, *p-GLUT4*, *GLUT4* in the brain of the tested objects

The tested objects were sacrificed by cervical dislocation to quickly remove its brain tissue, and the bilateral hippocampus and prefrontal cortex of which were separated on ice. After being labeled, they were placed in liquid nitrogen for quick freezing, and finally stored in a -80 °C refrigerator for testing. The extraction of total RNA was done with Trizol reagent. RNA integrity was detected by 2% agarose gel; the ratio of OD₂₆₀ to OD₂₈₀ indicates RNA purity. The extraction of total protein was extracted with RIPA reagent. The BCA method was used for protein quantification for Western Blot experiments. According to the experiment, the primer sequences are as following:

IRS-2: forward primer (5'-3') 19 bp: ATGGTGGCGAGGACAGTAG; reverse primer (5'-3'): GGGCTCAATGCTAGACGAGA.

PI3K: forward primer (5'-3'); 22 bp: ACTTTGTGATCTCCGCTT; reverse primer (5'-3'): TCCTGTATTCAGGATCATTAA.

AKT: forward primer (5'-3'); 20 bp: AAAGAGCGCATGAGTGACG; reverse primer (5'-3'): CGTGGTCTCTTGTAGTAG.

GLUT4: forward primer (5'-3'); 17 bp: CGAGGAAAGAATTAGGC; reverse primer (5'-3'): GTGGGGAATGTGAGCAG;

GAPDH: forward primer (5'-3'); 20 bp: CAAGAAGGTGGTGAAGCAGG; reverse primer (5'-3'): AAAGTGGAGGAGTGGGTGT.

The reverse transcription was done with the fast Quant RT kit (with g DNase) produced by Beijing Tiangen Biochemical Technology Co., Ltd. *Reaction conditions*: The samples were kept at the temperature of 42 °C first. After 15 min, the samples were transferred to 95 °C and stayed for 3 min. The obtained DNA stayed under the temperature of -20 °C. *PCR reaction system*: 2 × Super Real Pre Mix Plus 10 µl; Primer 1.2 µl; cDNA 2 µl; 50 × ROX Reference Dye 2 µl; Total 20 µl. *Conditions for Reacting*: 15 min at the temperature of 95 °C for pre-denaturation, then 10 s at 95 °C for denaturation, then annealing for 31 s at the temperature of 60 °C/extension, 40 cycles. Group C was set to be standard 1, and the relative quantitative value (RQ value) of the expression level of target genes were calculated with formula of $RQ = 2^{-\Delta\Delta Ct}$. The RQ value was for statistical analysis.

2.4. Statistical analysis

Analysis report was conducted in SPSS 17.0. The used indicators were mean ± standard error, as Mean ± SEM. Repeated measure-

ment analysis of variance (as repeated measurement ANOVA) were used to analyze the statistical indicators of the Morris Water Maze spatial acquisition experiments and working memory detection. The repeated measurement ANOVA and the LSD (Least Significant Difference) were carried to contrast the tested objects. Two-way ANOVA (as Analysis of Variance) was applied in the Morris Water Maze memory statistical analysis and the LSD test.

3. Results

3.1. Behavioral changes in Morris Water Maze test

3.1.1. Morris Water Maze test positioning and navigation ability in each group

In the navigational experiment of the water maze, the latency of the rats was gradually shortened as the training processed to reach the stage for each group. On Day 4, all rats in three groups can reach the platform in a short time after they were released into the water. In other words, they have memorized the position of the platform. As shown in Fig. 1, the latency of Day 5 and Day 4 did not differ dramatically. There were no remarkable changes on the latency of each group of animals on the same day. All groups had a shorter latency on Day 5 than on Day 1 ($P < 0.05$). Thus, it showed that all of them had formed the memory of the platform position after training. Refer to Table 1.

3.1.2. Morris water maze test space exploration experiment results of each group of rats' behaviors

On Day 3, after the surgery, Group S+L (100 $\mu\text{g}/\text{Kg}$) was shorter than Group C, L and S in the average target quadrant residence time, and lower than Group C in average number of perforations. The difference was obvious ($P < 0.05$). The average swimming speed among the groups is of no flagrant contrast ($P > 0.05$). Refer to Tables 2, 3, Figs. 2, 3.

In according to the mean target quadrant retention time, mean number of passages or average swimming speed among the groups on Day 7 after the surgery, no evident difference was displayed ($P > 0.05$). Refer to Table 3, Fig. 3.

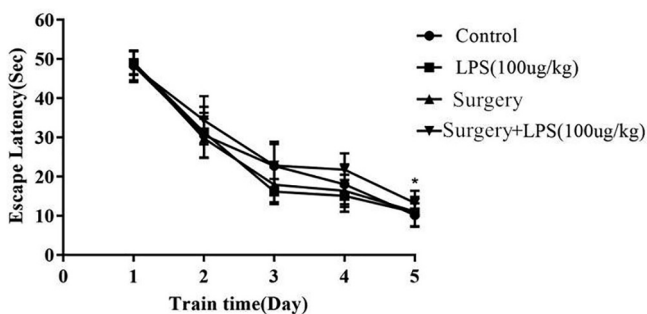


Fig. 1. Morris Water Maze test positioning flight test average latency of 5 days (sec). The platform latency on Day 5 was significantly shorter than on the first day of training ($P < 0.05$).

Table 1

Morris water maze test positioning time of the rats in each group of staging time (latency) ($\bar{x} \pm S$).

Train time (Day)	Control	LPS (100 $\mu\text{g}/\text{kg}$)	Surgery	Surgery + LPS (100 $\mu\text{g}/\text{kg}$)
1	48.32 ± 3.75	49.03 ± 3.05	49.16 ± 3.05	48.07 ± 3.97
2	30.58 ± 5.72	31.34 ± 6.52	29.76 ± 5.01	34.36 ± 6.15
3	22.72 ± 6.19	16.18 ± 3.19	17.94 ± 4.47	22.81 ± 5.53
4	18.04 ± 5.12	15.07 ± 4.06	16.38 ± 4.09	21.77 ± 4.16
5	10.15 ± 3.03	10.88 ± 3.56	11.08 ± 3.75	13.25 ± 3.11

Table 2

Behavior of SD rats in the Morris water maze test space exploration experiment (3 days after surgery) ($\bar{x} \pm S$).

Groups	3 days after surgery		
	Time in the target quadrant (sec)	Crossing	Swimming speed (m/s)
C	29.45 ± 3.01	3.32 ± 1.15	0.24 ± 0.08
L	28.76 ± 4.56	2.75 ± 0.94	0.21 ± 0.05
S	28.11 ± 3.78	2.83 ± 0.76	0.27 ± 0.07
S+L (100 $\mu\text{g}/\text{Kg}$)	19.77 ± 4.19 ^{a, b, c}	2.42 ± 0.77 ^a	0.26 ± 0.09

^a $P < 0.05$, compared with Group C.

^b $P < 0.05$, compared with Group L.

^c $P < 0.05$, compared with Group S.

Table 3

Behavior of SD rats in the Morris water maze test space exploration experiment (7 days after surgery) ($\bar{x} \pm S$).

Groups	7 days after surgery		
	Time in the target quadrant (sec)	Crossing	Swimming speed (m/s)
C	28.12 ± 6.36	2.96 ± 0.74	0.27 ± 0.06
L	26.53 ± 7.11	2.88 ± 0.87	0.22 ± 0.07
S	27.09 ± 8.43	2.91 ± 0.83	0.23 ± 0.08
S+L (100 $\mu\text{g}/\text{Kg}$)	25.31 ± 6.05	2.67 ± 0.74	0.26 ± 0.06

3.1.3. Behavioral results of working memory test

Results shown in the 3-day working memory test refers that the average latency of Group S+L (100 $\mu\text{g}/\text{Kg}$) was longer ($P < 0.05$). The average latency in Group L and S was longer than in Group C ($P > 0.05$). See from the 7-day working memory test, the average latency of the rats in Group L, S and S+L (100 $\mu\text{g}/\text{Kg}$) was longer than in Group C ($P > 0.05$). Refer to Tables 4, 5, and Figs. 4 and 5.

3.2. 18F-FDG PET/CT for detecting changes in glucose metabolism

Compared with preoperative rats, POCD rats of Group S+L (100 $\mu\text{g}/\text{Kg}$) were identified by 18F-FDG PET/CT three day later after the operation. The SUV_{max} of the frontal and temporal lobe areas has decreased significantly ($P < 0.05$). However, no evident difference was shown between Group C and the preoperative SUV_{max} ($P > 0.05$). Refer to Table 5, Figs. 5, 6.

3.3. Expression of PI3K (1:500), IRS-2 (1:200), AKT (1:250), and GLUT4 (1:500) related genes and protein factors in brain insulin signaling pathway

Compared with the characteristics of PI3K, IRS-2, AKT, and GLUT4 mRNA in the hippocampus of the Group C, the key genes of insulin signaling pathways in POCD rats were reduced in the level of expression. Refer to Fig. 7.

The expression of total protein of PI3K, IRS-2, GLUT4, and AKT in POCD rats was not contrastive from Group C. Yet the phosphorylation level has increased in IRS-2 protein. While, the phosphorylation levels decreased in PI3K, AKT and GLUT4 proteins. The

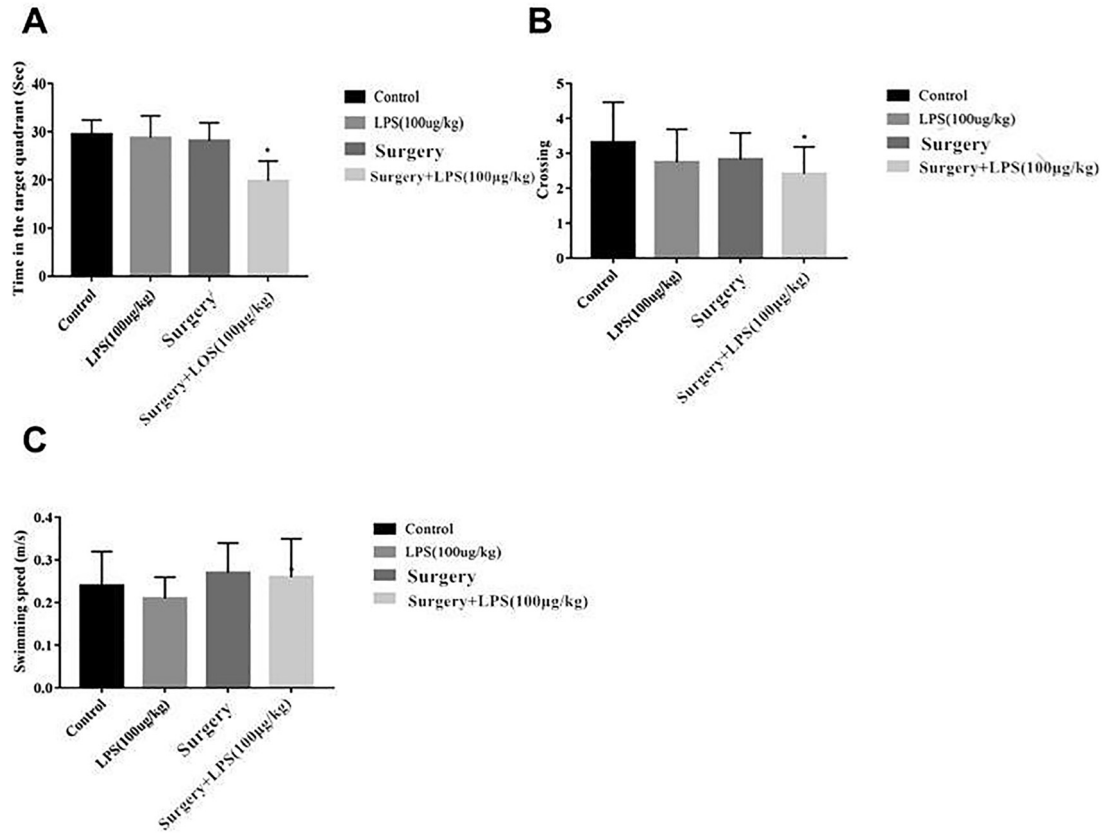


Fig. 2. Behavior of SD rats in the Morris water maze test space exploration experiment (3 days after the surgery). A: average target quadrant stay time; B: average number of passes; C: average swim speed. * $P < 0.05$ compared with Group C.

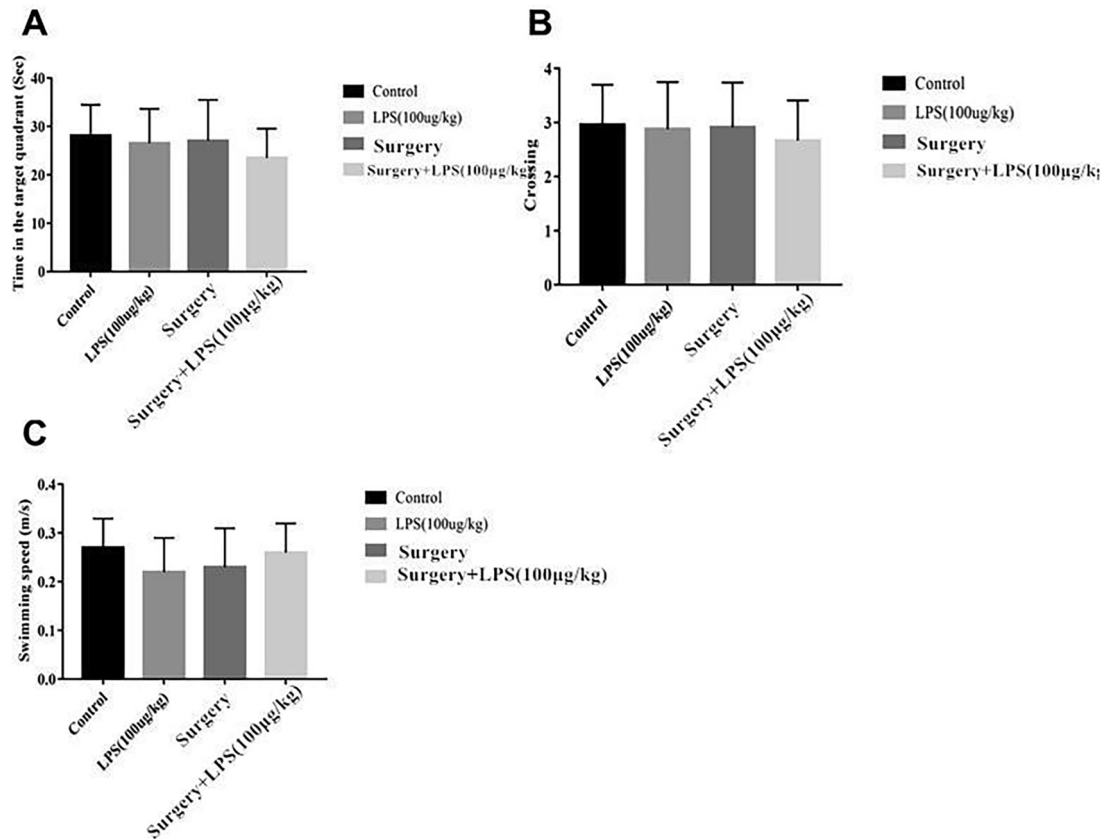


Fig. 3. Behavior of SD rats in the Morris water maze test space exploration experiment (7 days after the surgery). (A) Average target quadrant stay time; (B) average number of passes; (C) average swim speed.

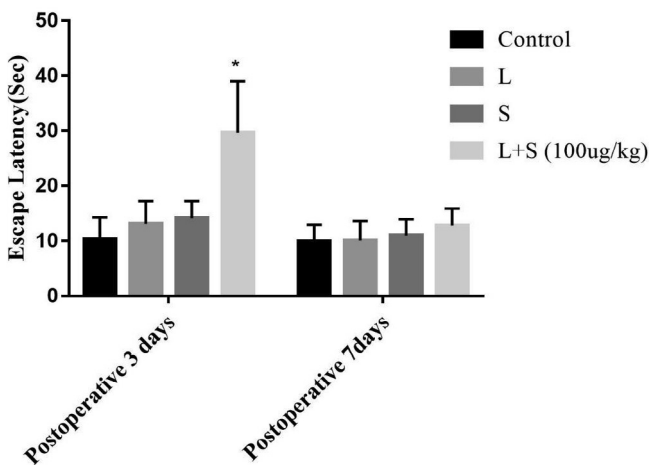
Table 4Behavior of rats in each group in Morris water maze test working memory experiment ($\bar{x} \pm S$).

Groups	Escape latency (sec)	
	Postoperative 3 days	Postoperative 7 days
C	10.41 ± 3.88	9.86 ± 3.07
L	13.09 ± 4.17	10.07 ± 3.52
S	14.15 ± 3.42	11.04 ± 2.88
S+L (100 µg/Kg)	29.64 ± 9.37 ^{a,b,c}	12.83 ± 3.06 ^a

^a $P < 0.05$, compared with Group C.^b $P < 0.05$, compared with Group L.^c $P < 0.05$, compared with Group S.**Table 5**

18F-FDG PET/CT of brain to detect glucose metabolism in brain of POCD rats.

Group	Pre-operation		Post-operation (3 days)	
	Frontal lobe	Temporal lobe	Frontal lobe	Temporal lobe
POCD	3.81 ± 0.39	3.62 ± 0.05	2.93 ± 0.28 ^a	2.84 ± 0.27 ^b
Control	3.58 ± 0.37	3.37 ± 0.12	3.77 ± 0.16	3.34 ± 0.08

^a $P < 0.05$, compared with Frontal lobe.^b $P < 0.05$, compared with Temporal lobe.**Fig. 4.** Morris water maze test behavioral memory test (3 and 7 days after the surgery). ^a $P < 0.05$, compared with Group C.

change is obviously seen ($P < 0.05$). This accords with the expression of the gene level. And, again it was verified that the insulin signaling pathway in the hippocampus of POCD rats has suffered from disorder, and the glucose metabolism of POCD rats becomes abnormal as well. Refer to Fig. 8.

4. Discussion

The clinical features of POCD can be manifested as loss of comprehension ability, inability to concentrate, memory loss, and decreased social ability, or anxiety, paralysis, and confusion. Studies have shown that hyperglycemia during extracorporeal circulation is an independent risk variable for POCD (Feinkohl et al., 2017b). Therefore, it is crucial to study on the mechanism of POCD caused by abnormal glucose metabolism.

Human brain only accounts for 2.5–3.0% of the body weight, but the cerebral blood flow accounts for 15–20% of the cardiac stroke volume. Brain is the largest oxygen consumer of the human body, which accounts for about 25% of the whole human body oxygen consumption, Glucose, transported through the blood and through

the blood-brain barrier into the cerebral circulation, serves as the dominant energy source in the brain. Glucose is then actively transported into the cell to produce ATP through aerobic oxidation or glycolysis pathways. Studies have shown that glucose metabolism disorder is one of the important pathological mechanisms of cognitive impairment (Zhao et al., 2018). It is also known that elevated blood glucose increases the toxicity of cytokines, leading to cognitive dysfunction in rats (Cukierman-Yaffe, 2014). Currently, possible mechanisms of abnormal glucose metabolism leading to POCD include: (1) insulin resistance (IR). IR also occurs during stress reactions such as trauma, shock, and infection, so IR is a marker of surgical stress. Since we know that the neuronal apoptosis, accompanied by the decrease in the number of neurons caused by cell necrosis, is one of the important causes of cognitive dysfunction, and as an important neurotrophic factor, insulin can promote the survival, growth and differentiation of neurons to protect damaged neurons and reduce their degradation. Therefore, IR greatly reduces the positive effect of insulin on cognitive function and might cause the occurrence of POCD (Ma et al., 2015). (2) Abnormal insulin signaling pathway. There are two pathways mainly included in insulin signaling pathway. One is PI3K, the phosphatidylinositol 3-kinase transmitting pathway. The other one is MAPK, as mitogen-activated protein kinase signaling pathway. The PI3K/AKT is a potential pathway for improving neuronal survival and differentiation during embryonic phase, responding to insulin and insulin-like growth factor and other inducing factors to maintain the balance of cell survival and apoptosis, and promote migration and myelination of neurons. (Liu et al., 2015). Maintaining normal brain blood homeostasis and energy metabolism depends on the normal functioning of the insulin signaling pathway, and abnormal insulin signaling pathways may result in reduced ATP production. Therefore, disruption of the insulin signaling pathway might severely impair learning and memory function (Bloemer et al., 2014). (3) Oxidative stress. Reactive oxygen species (ROS) acts indispensably in synaptic function in the brain. When the leverage between ROS production and intracellular antioxidants is severely disrupted, it would lead to mitochondrial dysfunction and cell damage. Abnormally elevated ROS can cause cognitive impairment (Hernandes et al., 2014). In addition, ROS activates the NF- κ B signaling pathway, which further activates PKC, leading to elevated advanced glycation end product (AGE), might result in impaired endothelial function (Toth et al., 2013). Stress response caused by surgical procedures and anesthesia operations might cause blood sugar fluctuations, which exacerbate oxidative stress, a possible mechanism for causing POCD (Steinthorsdottir et al., 2017). (4) abnormal blood-brain barrier. The blood-brain barrier has certain selectivity for the solute entering the brain to prevent it from being damaged by harmful substances in the blood circulation, and thus maintaining the basic stability of the brain environment. Abnormal glucose metabolism might damage the blood-brain barrier through multiple pathways. For example, insulin resistance leads to an increase in blood sugar, and hyperglycemia induces capillary proliferation, resulting in increased blood-brain barrier permeability. Abnormal glucose metabolism leads to decreased amount of materials transported through the blood-brain barrier, resulting in reduced transportation of trophic factors, including insulin, and thus puts the brain in an insulin-deficient environment, leading to decreased cognitive function (Lin et al., 2018; González-Reyes et al., 2016). (5) Glucose transporter 4 (GLUT4). GLUT4 is a class of membrane integrin proteins with 12 transmembrane domains involved in glucose uptake. The IRS-PI3K-AKT-GLUT4 signaling pathway is the most likely signal transduction pathway for insulin activities in the central nervous system. Under the condition of resting state, GLUT4 is mainly stored in the vesicles of the cells, and the vesicles are transported to the cell membrane when stimulated. GLUT4 fused into

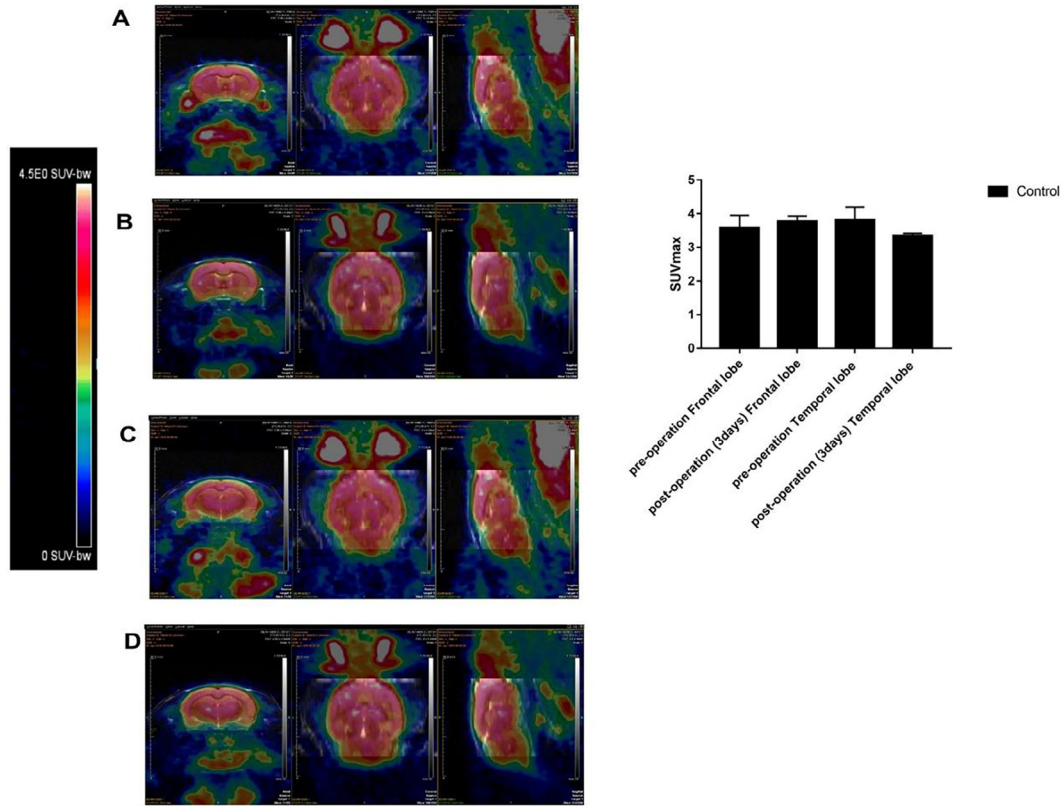


Fig. 5. ¹⁸F-FDG PET/CT imaging to identify changes in glucose metabolism in the brain of C group. (A) Changes in SUV_{max} of preoperative rats' frontal lobe; (B) changes in SUV_{max} of frontal lobe 3 days after the surgery; (C) changes in SUV_{max} of temporal lobe before the surgery; (D) changes in SUV_{max} of temporal lobe 3 days after the surgery.

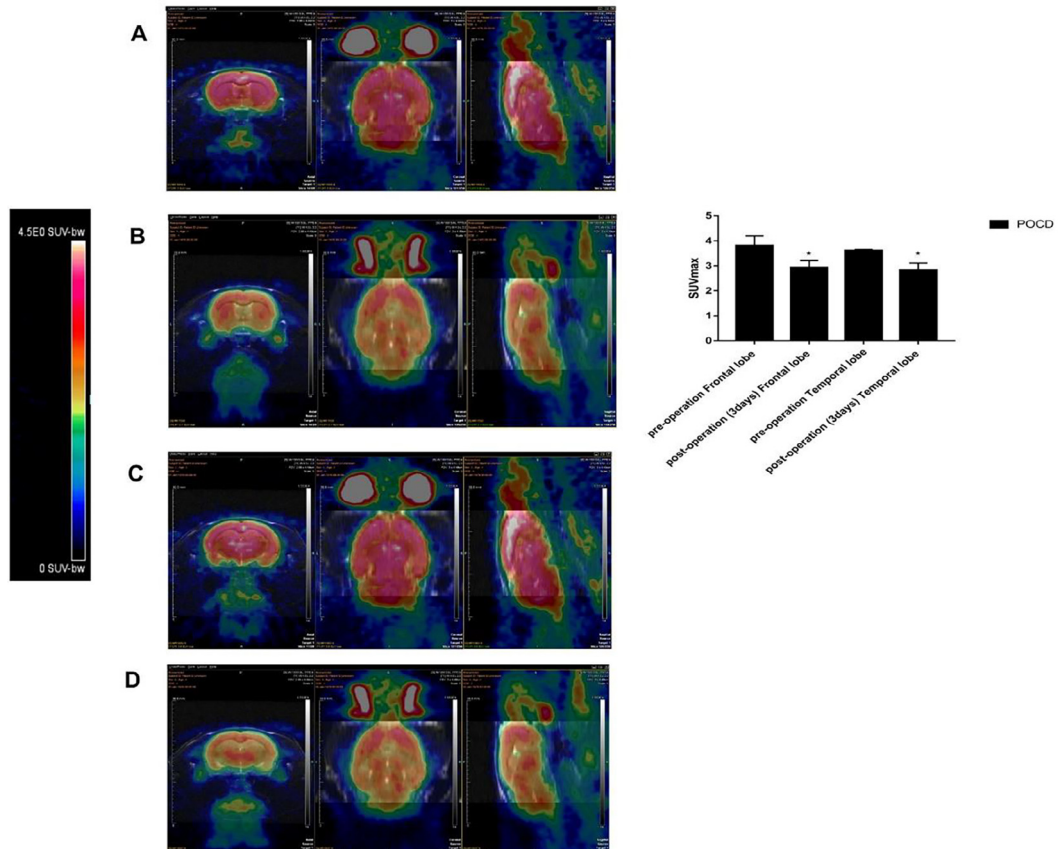


Fig. 6. ¹⁸F-FDG PET/CT of brain to identify changes in glucose metabolism in POCD rats. (A) Changes in SUV_{max} of preoperative rats' frontal lobe; (B) changes in SUV_{max} of frontal lobe 3 days after the surgery; (C) changes in SUV_{max} of temporal lobe before the surgery; (D) changes in SUV_{max} of temporal lobe 3 days after the surgery.

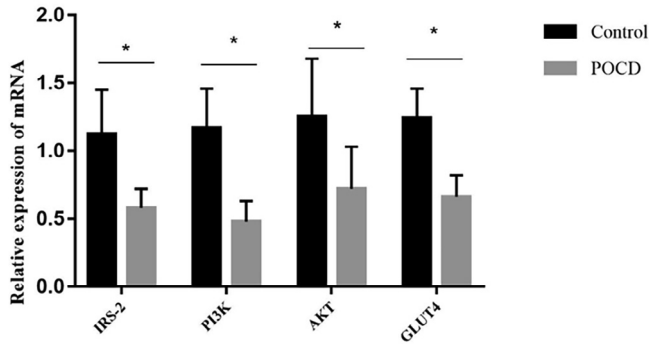


Fig. 7. Expression of IRS-2-PI3K-AKT-GLUT4 related genes in the insulin signaling pathway of POCD rats.

the cell membrane can increase glucose uptake. Therefore, this signaling pathway disorder may correlate with neuronal glucose metabolism and cognitive function changes (Ramachandran and Saravanan, 2015; Yu et al., 2017).

In this study, unilateral nephrectomy as well as 100 µg/kg LPS intraperitoneal injection is applied to set cognitive dysfunction models in adult SD rats, and the results of Morris Water Maze test will evaluate the POCD status of the rats. Statistical analysis showed the objects assigned to Group S+L statistically significant behavioral changes in the spatial exploration test and the learning working memory test, while others did not. This suggests that adult rats with only surgical stimulation, intraperitoneal injection of LPS, or intraoperative intraperitoneal injection of small doses of LPS is not enough to cause cognitive dysfunction. Studies have reported that rodents go through the surgery may experience cognitive impairment, which might be a result of high conditions of

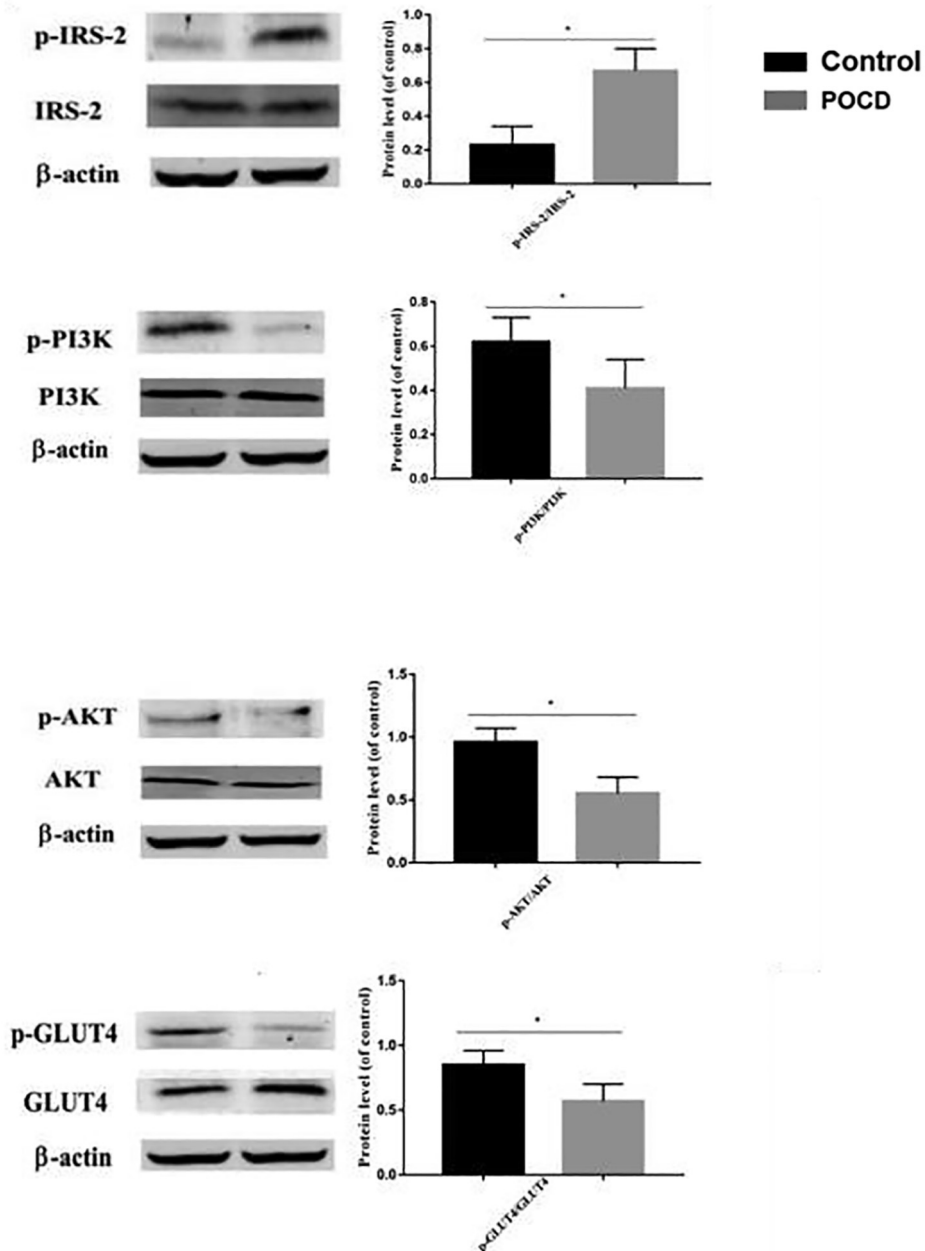


Fig. 8. The Expression of IRS-2-PI3K-AKT-GLUT4 related genes in the insulin signaling pathway of POCD rats.

inflammatory factors in the peripheral and brain caused by surgical stimulation. The infection of the peripheral system also increases the level of inflammatory factors in the brain, and thus aggravating postoperative cognitive dysfunction.

Presently, it has been recognized internationally that 18F-FDG PET/CT is efficient in finding brain glucose metabolism-related damage in neurodegenerative dementia. Normal brain cells have high metabolism of 18F-FDG, while regional glucose metabolism does not. The characteristic pattern can be used to distinguish vascular cognitive dysfunction in early stage. The standard uptake value (SUV) is, in this study, a quantitative index to reflect the degree of glucose concentration in brain cells, which means it can reflect the metabolic level of brain cells (Zhang et al., 2016). Therefore, it is vital for diagnosis of dementia, both early and differential. The local metabolic abnormality of 18F-FDG PET/CT is called 'nerve'. One major feature of neurodegenerative dementia is the presence of downstream biomarkers of meta-injury (Grassetto et al., 2014; Tripathi et al., 2014). According to this study, compared with preoperative rats, POCD rats of Group S+L (100 µg/Kg) were identified by 18F-FDG PET/CT in three days of the operation. The SUV_{max} of the frontal and temporal lobe regions has decreased. Group C showed no significant difference from the preoperative rats in SUV_{max}, which indicates that Group S+L suffered from cognitive dysfunction caused by abnormalities in glucose metabolism. This also shows that as a new functional imaging technology, 18F-FDG PET/CT provides good technical support and auxiliary methods for early diagnosis of POCD.

In addition, the expression of IRS-PI3K-AKT-GLUT4 related genes and protein factors was detected in the brain insulin signaling pathway of POCD rats. Results indicated that the key genes of insulin signaling pathways in the POCD rats hippocampus were mainly PI3K, IRS-2, and AKT, out from the expression of PI3K, IRS-2, GLUT4 and AKT mRNA in the hippocampus of Group C. what's more, the expression level of GLUT4 mRNA is lower than the preoperative rats. Total protein expression of PI3K, IRS-2, GLUT4 and AKT in the POCD rats was indistinctive from that in Group C. The phosphorylation level is higher in IRS-2 protein of the POCD rats than that of Group C, while it is lower in PI3K, AKT and GLUT4 proteins. Consistent with the expression of the gene level, it was confirmed that the insulin signaling pathway is abnormal in the hippocampus of POCD rats, as well as its glucose metabolism.

5. Conclusion

4.1 The unilateral nephrectomy and injection of LPS (100 µg/kg) was applied to prepare the cognitive dysfunction model of adult SD rats.

4.2 18F-FDG PET/CT imaging technique could work efficiently for early diagnosis of brain metabolic abnormalities in POCD rats;

4.3 Metabolic abnormalities in the brain of POCD rats are related with abnormal expression of IRS-PI3K-AKT-GLUT4 related genes and protein factors in the insulin signaling pathway.

6. Authors' contributions

YD, ZX and WM have full access to the database in this study. Study design: YD, HC, ZX, WM. Acquisition of data: RD, HC, YX, JL, ES, ZX. Analysis and interpretation of data: YD, NT, YJ, LS, YS, YW, JW, JZ, QY. Manuscript preparation: YD and ZX. Statistical analysis: YD, HC and ZX. The authors listed have fully read and consented to the final manuscript version.

Declaration of Competing Interest

None conflict of financial interest was claimed by the author.

Acknowledgements

Sincere appreciation to Weidong Mi and Zhipeng Xu, funded by the National Natural Science Foundation of China (81371204, 81671039, 81471119) respectively.

References

- Banzo, I., Jiménez-Bonilla, J., Ortega-Nava, F., Quirce, R., Martínez-Rodríguez, I., de Arcocha-Torres, M., Rodríguez, E., Vázquez, J.L., Sánchez, P.J., Martínez-Amador, N., Ibañez-Bravo, S., Carril, J.M., 2014. Amyloid imaging with (11)C-PIB PET/CT and glucose metabolism with (18)F-FDG PET/CT in a study on cognitive impairment in the clinical setting. *Nucl. Med. Commun.* 35 (3), 238–244.
- Bloemer, J., Bhattacharya, S., Amin, R., Suppiramaniam, V., 2014. Impaired insulin signaling and mechanisms of memory loss. *Prog. Mol. Biol. Transl. Sci.* 121, 413–449.
- Carr, Z.J., Cios, T.J., Potter, K.F., Swick, J.T., 2018. Does dexmedetomidine ameliorate postoperative cognitive dysfunction? A brief review of the recent literature. *Curr. Neurol. Neurosci. Rep.* 18 (10), 64.
- Casella, M., Bimonte, S., 2017. The role of general anesthetics and the mechanisms of hippocampal and extra-hippocampal dysfunctions in the genesis of postoperative cognitive dysfunction. *Neural Regen. Res.* 12 (11), 1780–1785.
- Cropsey, C., Kennedy, J., Han, J., Pandharipande, P., 2015. Cognitive dysfunction, delirium, and stroke in cardiac surgery patients. *Semin. Cardiothorac. Vasc. Anesth.* 19 (4), 309–317.
- Cukierman-Yaffe, T., 2014. Diabetes, dysglycemia and cognitive dysfunction. *Diabetes Metab. Res. Rev.* 30 (5), 341–345.
- Díaz-Venegas, C., Schneider, D.C., Myrskylä, M., Mehta, N.K., 2017. Life expectancy with and without cognitive impairment by diabetes status among older Americans. *PLoS ONE* 12 (12), e0190488.
- Feinkohl, I., Winterer, G., Spies, C.D., Pischon, T., 2017a. Cognitive reserve and the risk of postoperative cognitive dysfunction. *Deutsch Arztebl. Int.* 114 (7), 110–117.
- Feinkohl, I., Winterer, G., Pischon, T., 2017b. Diabetes is associated with risk of postoperative cognitive dysfunction: a meta-analysis. *Diabetes Metab. Res. Rev.* 33 (5).
- Fischer, I., Alliod, C., Martinier, N., Newcombe, J., Brana, C., Pouly, S., 2011. Sphingosine kinase 1 and sphingosine 1-phosphate receptor 3 are functionally upregulated on astrocytes under pro-inflammatory conditions. *PLoS ONE* 6 (8), e23905.
- González-Reyes, R.E., Aliev, G., Ávila-Rodríguez, M., Barreto, G.E., 2016. Alterations in glucose metabolism on cognition: a possible link between diabetes and dementia. *Curr. Pharm. Des.* 22 (7), 812–818.
- Grassetto, G., Marzola, M.C., Musto, A., Viniamury, S., Colletti, P.M., Perkins, A.C., Rubello, D., 2014. Non-Alzheimer types of neurodegenerative dementia: clinical and 18F-FDG-PET/CT pictures. *Nucl. Med. Commun.* 35 (11), 1085–1092.
- Hernandes, M.S., D'Ávila, J.C., Trevelin, S.C., Reis, P.A., Kinjo, E.R., Lopes, L.R., Castro-Faria-Neto, H.C., Cunha, F.Q., Britto, L.R., Bozza, F.A., 2014. The role of Nox2-derived ROS in the development of cognitive impairment after sepsis. *J. Neuroinflammation* 11, 36.
- Jiménez-Bonilla, J.F., Banzo, I., De Arcocha-Torres, M., Quirce, R., Martínez-Rodríguez, I., Lavado-Pérez, C., Bravo-Ferrer, Z., Rodríguez-Rodríguez, E., Sánchez-Juan, P., Carril, J.M., 2016. Diagnostic role of 11C-Pittsburgh compound B retention patterns and glucose metabolism by fluorine-18-fluorodeoxyglucose PET/CT in amnesic and nonamnesic mild cognitive impairment patients. *Nucl. Med. Commun.* 37 (11), 1189–1196.
- Jones, P., 2008. Perioperative glycemic control and postoperative cognitive dysfunction: an expression of caution. *Can. J. Anaesth.* 55 (8), 559–560.
- Lin, Y., Wang, K., Ma, C., Wang, X., Gong, Z., Zhang, R., Zang, D., Cheng, Y., 2018. Evaluation of metformin on cognitive improvement in patients with non-dementia vascular cognitive impairment and abnormal glucose metabolism. *Front. Aging Neurosci.* 10, 227.
- Liu, C.C., Hu, J., Tsai, C.W., Yue, M., Melrose, H.L., Kanekiyo, T., Bu, G., 2015. Neuronal LRP1 regulates glucose metabolism and insulin signaling in the brain. *J. Neurosci.* 35 (14), 5851–5859.
- Ma, L., Wang, J., Li, Y., 2015. Insulin resistance and cognitive dysfunction. *Clin. Chim. Acta* 444, 18–23.
- McNay, E.C., Recknagel, A.K., 2011. Brain insulin signaling: a key component of cognitive processes and a potential basis for cognitive impairment in type 2 diabetes. *Neurobiol. Learn. Mem.* 96 (3), 432–442.
- Needham, M.J., Webb, C.E., Bryden, D.C., 2017. Postoperative cognitive dysfunction and dementia: What we need to know and do. *Br. J. Anaesth.* 119 (suppl_1), i115–i125. An excellent analysis of the definition and diagnosis of postoperative cognitive dysfunction.
- Pearson-Leary, J., McNay, E.C., 2016. Novel roles for the insulin-regulated glucose transporter-4 in hippocampally dependent memory. *J. Neurosci.* 36 (47), 11851–11864.
- Ramachandran, V., Saravanan, R., 2015. Glucose uptake through translocation and activation of GLUT4 in PI3K/Akt signaling pathway by asiatic acid in diabetic rats. *Hum. Exp. Toxicol.* 34 (9), 884–893.
- Rizzo, M.R., Barbieri, M., Boccardi, V., Angellotti, E., Marfella, R., Paolisso, G., 2014. Dipeptidyl peptidase-4 inhibitors have protective effect on cognitive

- impairment in aged diabetic patients with mild cognitive impairment. *J. Gerontol. A Biol. Sci. Med. Sci.* 69 (9), 1122–1131.
- Sochocka, M., Sobczyński, M., Sender-Janeczek, A., Zwolińska, K., Błachowicz, O., Tomczyk, T., Ziętek, M., Leszek, J., 2017. Association between periodontal health status and cognitive abilities. The role of cytokine profile and systemic inflammation. *Curr. Alzheimer Res.* 14 (9), 978–990.
- Steinmetz, J., Rasmussen, L.S., 2016. Peri-operative cognitive dysfunction and protection. *Anaesthesia* 71 (Suppl 1), 58–63.
- Steinhorsdottir, K.J., Kehlet, H., Aasvang, E.K., 2017. Surgical stress response and the potential role of preoperative glucocorticoids on post-anesthesia care unit recovery. *Minerva Anestesiol.* 83 (12), 1324–1331.
- Toth, P., Csiszar, A., Sosnowska, D., Tucsek, Z., Cseplo, P., Springo, Z., Tarantini, S., Sonntag, W.E., Ungvari, Z., Koller, A., 2013. Treatment with the cytochrome P450 ω -hydroxylase inhibitor HET0016 attenuates cerebrovascular inflammation, oxidative stress and improves vasomotor function in spontaneously hypertensive rats. *Br. J. Pharmacol.* 168 (8), 1878–1888.
- Tripathi, M., Tripathi, M., Damle, N., Kushwaha, S., Jaimini, A., D'Souza, M.M., Sharma, R., Saw, S., Mondal, A., 2014. Differential diagnosis of neurodegenerative dementias using metabolic phenotypes on F-18 FDG PET/CT. *Neuroradiol. J.* 27 (1), 13–21.
- Yaffe, K., Lindquist, K., Schwartz, A.V., Vitartas, C., Vittinghoff, E., Satterfield, S., Simonsick, E.M., Launer, L., Rosano, C., Cauley, J.A., Harris, T., 2011. Advanced glycation end product level, diabetes, and accelerated cognitive aging. *Neurology* 77 (14), 1351–1356.
- Yu, N., Fang, X., Zhao, D., Mu, Q., Zuo, J., Ma, Y., Zhang, Y., Mo, F., Zhang, D., Jiang, G., Wu, R., Gao, S., 2017. Anti-diabetic effects of Jiang Tang Xiao Ke Granule via PI3K/Akt signalling pathway in type 2 diabetes KKAY Mice. *PLoS ONE* 12 (1).
- Zhang, W., Ning, N., Li, X., Niu, G., Bai, L., Guo, Y., Yang, J., 2016. Changes of brain glucose metabolism in the pretreatment patients with non-small cell lung cancer: a retrospective PET/CT study. *PLoS ONE* 11 (8), e0161325.
- Zhao, M., Yuan, M.M., Yuan, L., Huang, L.L., Liao, J.H., Yu, X.L., Su, C., Chen, Y.H., Yang, Y.Y., Yu, H., Xu, X., 2018. Chronic folate deficiency induces glucose and lipid metabolism disorders and subsequent cognitive dysfunction in mice. *PLoS ONE* 13 (8), e0202910.